

Nonmodal instability of a stratified plane-channel suspension flow with fine particlesSergei A. Boronin^{1,2,*} and Alexander N. Osipov²¹*Schlumberger Moscow Research, Pudovkina 13, 119285 Moscow, Russia*²*Institute of Mechanics, M.V. Lomonosov Moscow State University, Michurinskii Prospect 1, 119192 Moscow, Russia*

(Received 29 November 2015; published 8 March 2016)

We consider the nonmodal instability and transient growth of small disturbances in a plane-channel suspension flow with a nonuniform concentration profile of fine noncolloidal particles accumulated in two localized layers, symmetric about the channel axis. A single-velocity model of an effective Newtonian fluid with a finite particle volume fraction is employed. It is established that fine particles distributed nonuniformly in the main flow significantly modify the growth rate of the first mode in a wide range of governing parameters. The most pronounced destabilizing effect is produced by the particles localized in the vicinity of the walls. A parametric study of the so-called optimal disturbances showed that they are streaks elongated in the flow direction, similar to the optimal disturbances in the flow devoid of particles. The transverse wave number of the optimal disturbances depends strongly on the location of the particle layers. Even when the particle mass concentration (averaged over the channel cross section) is small (of the order of a percent) and the particles are localized in the middle between the walls and the channel axis, the energy of the optimal disturbances is by several orders of magnitude larger than in dusty-gas and pure-fluid flows. When the particle layers are located in the vicinity of the walls or the channel axis, the nonmodal instability mechanism is less pronounced, as compared to the flow devoid of particles.

DOI: [10.1103/PhysRevE.93.033107](https://doi.org/10.1103/PhysRevE.93.033107)**I. INTRODUCTION**

The laminar-turbulent transition is one of the most important problems associated with the disperse flows encountered in a variety of industrial and technological processes. The number of existing experimental studies on the subject is very limited [1], so that theoretical investigations are required to study the effect of particles on the stability of shear flows. It will provide a basis for experimental investigations and make it possible to formulate recommendations on the improvement of existing technological solutions.

The stability of particle-laden flows was analyzed mostly within the framework of a classical (modal) approach [2,3]. In accordance with this approach, for a given set of governing parameters the flow is assumed to be unstable if there exists at least one growing normal mode. The first formulation of the linear stability problem for a particle-laden flow was given by Saffman [4] in the framework of a dusty-gas model with Stokesian particles and a uniform distribution of the dispersed phase, having negligibly small volume fraction, in the main flow. Later, the formulation was modified and a number of additional factors, important for real particle-laden flows, were considered: the nonuniform particle concentration profile [5,6], non-Stokesian components of the interphase force [6], and finite volume fraction of particles [7,8]. It was found that the presence of both a finite and an infinitely small volume fraction of inertial particles may significantly affect the growth rate of the first mode, which not only changes the critical Reynolds number, but also triggers new instability mechanisms. A thorough overview of the studies on the modal stability of particle-laden flows can be found, for example, in [6,7,9].

In 1970–1980, it was demonstrated that in any shear flow there exist streamwise-independent disturbances which in

contrast to the exponential temporal behavior predicted by the classical theory, grow linearly with time [10,11]. This algebraic instability mechanism is inviscid in nature, so that even at subcritical Reynolds numbers certain disturbances can grow enough to trigger the laminar-turbulent transition or the secondary instability [12]. Mathematically, the nonexponential growth of disturbances is attributable to the non-Hermitian property of the differential operators describing the evolution of small disturbances in shear flows. There exists a certain linear combination of decaying three-dimensional normal modes whose energy grows up and, at a certain finite instant of time, becomes by several orders of magnitude larger than its initial value. The algebraic growth is limited in time, so that at large times the evolution of the linear combination of normal modes is determined by the mode with the largest growth rate.

The general method of studying the algebraic instability is based on the analysis of the so-called “optimal disturbances,” which are linear combinations of normal modes with the largest energy growth on the time interval considered. The global optimal disturbances are optimized with respect to not only the initial conditions, but also to the value of the time interval and wave numbers. The global optimal disturbances were studied for all typical shear flows of pure fluid [13–17]. It was found that the optimal disturbances are “streaks,” i.e., streamwise-elongated periodic structures which are usually observed in experiments on laminar-turbulent transition [18].

Nonmodal instability in two-phase flows was studied for several dispersed flows within the framework of a two-fluid model with negligibly small particle volume fraction [19–21] and a finite volume fraction [22]. In [19], the optimal disturbances of a plane-channel dusty-gas flow were analyzed, assuming that the interphase momentum exchange is described by the Stokes force and the particle concentration in the main flow is uniform. It is shown that, with an increase in the particle mass loading α , the energy of optimal disturbances increases

*Corresponding author: sergeyboronin@yandex.ru

by the factor $(1 + \alpha)^2$, with the optimal time interval increasing linearly with α . The shape of the optimal disturbances in the dusty-gas flow turned out to be identical to that of the flow devoid of particles. Additional interphase forces (added mass, Basset-Boussinesq, and Archimedes) and a finite particle volume fraction do not significantly affect the parameters of optimal disturbances of the uniform suspension flow in a plane channel as compared to the pure-fluid flow [22].

In real particle-laden shear flows, the particle concentration profile in the main flow is usually very nonuniform due to the action of shear-induced lifting forces on the particles. The effect of this nonuniformity on optimal disturbances to dusty-gas flows in a plane-channel and boundary layer was analyzed in Refs. [20] and [21], respectively. In those studies, the particles were assumed to be localized in two layers with the Gaussian concentration profiles, symmetric with respect to the channel axis, and in a single layer in the boundary layer flow. It was found that, for a fixed average particle mass concentration, the largest energy of optimal disturbances corresponds to the flow with narrow particle layers located in the middle between the channel walls and the axis, or approximately in the middle of the boundary layer thickness. Even for moderate average particle mass concentration (about 10%), the maximum energy of the optimal disturbances of dusty-gas flow is several times larger than that in the pure-fluid flow.

In suspension flows, where particle-to-carrier fluid substance density ratio is of order unity and the mass concentration of the particles is not negligibly small, it is necessary to take into account the effects of finite particle volume fraction. Nonuniformly distributed particles modify the main flow velocity profile, since the effective suspension viscosity is the function of particle volume fraction. As shown in [8,23], a nonuniform distribution of the particle volume concentration in the main flow results in the onset of a new instability mechanism (viscous analog of Kelvin-Helmholtz instability), triggered even at small and moderate Reynolds numbers.

In the present study, we aimed at analyzing the effect of nonuniform distribution of particles on the transient growth and energy of optimal disturbances in a plane-channel suspension flow with a finite particle volume fraction. It is assumed that, in the main flow, the particles are accumulated in two localized layers, symmetric with respect to the channel axis. Such particle concentration distributions are typical of real suspension flows in ducts due to the so-called ‘‘tubular pinch effect’’ [24,25].

II. SUSPENSION FLOW MODEL

We consider an isothermal suspension flow in a plane channel. To clarify the formulation of the model of an effective stratified medium, which will be used for studying the stability problem, we start with the formulation of a general two-fluid approach [7,26] under the assumption of a small but finite particle volume fraction. The carrier fluid is Newtonian and incompressible, and the dispersed phase consists of identical non-Brownian particles.

The equations of the two-fluid model of suspension flow in dimensionless form are as follows:

$$\operatorname{div}[(1 - C)\mathbf{v} + C\mathbf{v}_s] = 0, \quad (1)$$

$$(1 - C)\frac{d\mathbf{v}}{dt} + \eta C\frac{d_s\mathbf{v}_s}{dt} = -\nabla p + \frac{1}{\operatorname{Re}}\nabla_j\tau^{ij}\mathbf{e}_i - \frac{1}{\operatorname{Fr}^2}[(1 - C) + \eta C]\mathbf{e}_2, \quad (2)$$

$$\frac{\partial C}{\partial t} + \operatorname{div}(C\mathbf{v}_s) = 0, \quad (3)$$

$$\frac{d_s\mathbf{v}_s}{dt} = \frac{1}{\operatorname{St}}(\mathbf{v} - \mathbf{v}_s)f(C) - \frac{1}{\operatorname{Fr}^2}\left(1 - \frac{1}{\eta}\right)\mathbf{e}_2, \quad (4)$$

$$\tau^{ij} = 2\mu(C)\left(e^{ij} - \frac{1}{3}\delta^{ij}\operatorname{div}\mathbf{v}\right),$$

$$e^{ij} = \frac{1}{2}(\nabla^i v^j + \nabla^j v^i), \quad \mu = 1 + \frac{5}{2}C, \quad \operatorname{Re} = \frac{U_0 L \rho^0}{\mu_0},$$

$$\operatorname{St} = \frac{mU_0}{6\pi\sigma\mu_0 L}, \quad \eta = \frac{\rho_s^0}{\rho^0}, \quad \operatorname{Fr}^2 = \frac{U^2}{gL}. \quad (5)$$

Here, ρ^0 and ρ_s^0 are the carrier fluid and particle substance densities, \mathbf{v} and \mathbf{v}_s are the carrier fluid and the particle velocities; C is the particle volume fraction; σ and m are the particle radius and mass; τ^{ij} and e^{ij} are the components of the viscous-stress and strain rate tensors; μ_0 and μ are the viscosities of the carrier fluid and suspension; δ^{ij} is the Kronecker δ ; \mathbf{e}_i are the basis vectors; and $f(C)$ is the correction to the Stokes force due to a finite volume fraction of particles. As the volume fraction of particles is assumed to be sufficiently small, we consider Einstein’s correction to the fluid viscosity (5). The flow scales involve the suspension velocity at the channel axis U_0 and the channel width L . The x axis of the Cartesian coordinate system is directed streamwise, the y axis is perpendicular to the channel walls, and the z axis is normal to the plane of velocity shear. The origin of the coordinate system is located at the channel axis (see Fig. 1). The set of nondimensional flow parameters involves the Reynolds number Re , the Stokes number St , the particle-to-fluid substance density ratio η , and the Froude number Fr . The material derivatives $d\mathbf{v}/dt$ and $d_s\mathbf{v}_s/dt$ are calculated along the trajectories of the phases:

$$\frac{d\mathbf{v}}{dt} = \frac{\partial\mathbf{v}}{\partial t} + (\mathbf{v}\nabla)\mathbf{v}, \quad \frac{d_s\mathbf{v}_s}{dt} = \frac{\partial\mathbf{v}_s}{\partial t} + (\mathbf{v}_s\nabla)\mathbf{v}_s.$$

In studying the stability problem, we will restrict our attention only to sufficiently fast ($\operatorname{Fr} \gg 1$) flows of suspension, laden with fine particles $\operatorname{St} \ll 1$. Under these simplifications, the system (1)–(4) turns into the following:

$$\operatorname{div}\mathbf{v} = 0, \quad [(1 - C) + \eta C]\frac{d\mathbf{v}}{dt} = -\nabla p + \frac{1}{\operatorname{Re}}\nabla_j\tau^{ij}\mathbf{e}_i, \quad (6)$$

$$\frac{\partial C}{\partial t} + \operatorname{div}(C\mathbf{v}) = 0, \quad \tau^{ij} = 2\mu(C)e^{ij}, \quad \mu = 1 + \frac{5}{2}C. \quad (7)$$

In the small-inertia limit, the particles modify the density and viscosity of the suspension. The suspension velocity is now nondivergent since the velocities of the phases are equal.

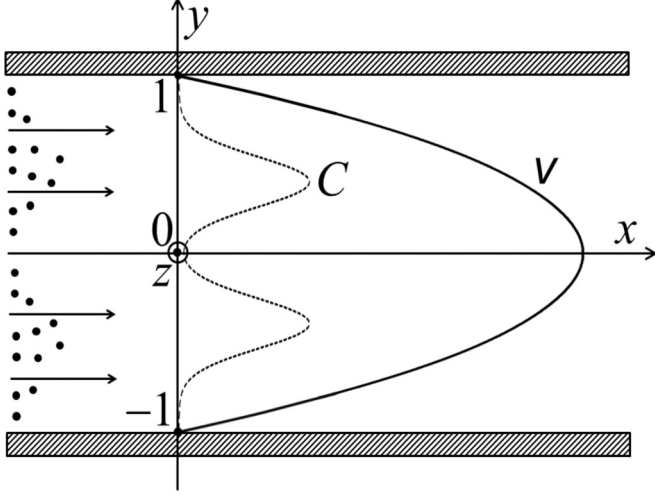


FIG. 1. Sketch of the suspension flow in a plane channel with a certain velocity profile v and a nonuniform particle volume concentration C .

III. LINEAR STABILITY AND OPTIMAL DISTURBANCES

Consider the suspension flow in a plane channel with the nonuniform distribution of particle volume fraction in the form of two symmetric layers similar to [5,20]

$$C_0(y) = \frac{\alpha}{\eta} C_* \left(\exp\left\{-\frac{(y-\zeta)^2}{\xi^2}\right\} + \exp\left\{-\frac{(y+\zeta)^2}{\xi^2}\right\} \right). \quad (8)$$

Here, the parameter ζ determines the location of the particle layer, while ξ determines its width. The scaling coefficient C_* satisfies the following relation:

$$C_* = \left(\frac{1}{2} \int_{-1}^1 \left(\exp\left\{-\frac{(y-\zeta)^2}{\xi^2}\right\} + \exp\left\{-\frac{(y+\zeta)^2}{\xi^2}\right\} \right) dy \right)^{-1}.$$

With this definition of C_* , the channel width-averaged particle volume concentration (8) equals α/η , so that α is the average mass loading. By varying η , one can study the effect of particle volume fraction on the flow stability at the fixed average particle mass loading α .

The main flow suspension velocity profile \mathbf{V} is determined by solving Eq. (6), assuming that there is no particle velocity slip $\mathbf{V}_s = \mathbf{V}$, the flow is horizontal $\mathbf{V} = \{U(y), 0, 0\}$ and applying the no-slip boundary conditions at the walls. Under these assumptions, the momentum conservation equation (6) is formulated as follows:

$$\frac{\partial p}{\partial x} = \frac{1}{\text{Re}} \frac{d}{dy} \{ \mu [C_0(y)] U' \}, \quad \frac{\partial p}{\partial y} = 0, \quad \frac{\partial p}{\partial z} = 0.$$

It follows from the equations above that the pressure is independent of y and z and depends linearly on x . Therefore, the velocity profile satisfies the following boundary-value problem for the ordinary differential equation,

$$\frac{d}{dy} \{ \mu [C_0(y)] U'(y) \} = l \text{Re}, \quad U(-1) = U(1) = 0, \quad (9)$$

where l is the pressure gradient in streamwise direction.

The equation above is solved numerically for a certain nonzero value of l (e.g., $l = 1$) using the fourth-order Runge-

Kutta method, and the resulting velocity profile is normalized, so that $U(0) = 1$.

We will now formulate the linear stability problem. The flow (8), (9) is subject to small three-dimensional disturbances:

$$\mathbf{v} = \mathbf{V} + \mathbf{v}', \quad C = C_0 + C', \quad p = P + p'.$$

The linearized system (6) and (7) is formulated as follows (in what follows, for simplicity we dropped the accent at disturbances):

$$\nabla \cdot \mathbf{v} = 0, \quad \frac{\partial C}{\partial t} + U \frac{\partial C}{\partial x} + v C'_0 = 0, \quad (10)$$

$$\rho_m \left(\frac{\partial u}{\partial t} + U \frac{\partial u}{\partial x} + U' v \right) = -\frac{\partial p}{\partial x} + \frac{1}{\text{Re}} \left\{ \frac{5}{2} (U' C)' + C'_0 \left(\frac{\partial u}{\partial y} + \frac{\partial v}{\partial x} \right) + \left(1 + \frac{5}{2} C_0 \right) \Delta u \right\}, \quad (11)$$

$$\rho_m \left(\frac{\partial v}{\partial t} + U \frac{\partial v}{\partial x} \right) = -\frac{\partial p}{\partial y} + \frac{1}{\text{Re}} \left\{ \frac{5}{2} U' \frac{\partial C}{\partial x} + 5 \frac{\partial v}{\partial y} C'_0 + \left(1 + \frac{5}{2} C_0 \right) \Delta v \right\}, \quad (12)$$

$$\rho_m \left(\frac{\partial w}{\partial t} + U \frac{\partial w}{\partial x} \right) = -\frac{\partial p}{\partial z} + \frac{1}{\text{Re}} \left\{ \frac{5}{2} C'_0 \left(\frac{\partial w}{\partial y} + \frac{\partial v}{\partial z} \right) + \left(1 + \frac{5}{2} C_0 \right) \Delta w \right\}, \quad (13)$$

$$\rho_m = (1 - C_0) + \eta C_0.$$

The linearized equations should satisfy the no-slip boundary conditions at the walls:

$$\mathbf{v}(y = \pm 1) = 0. \quad (14)$$

Note that despite the simplifying assumption of the negligibly small particle inertia, the disturbance of the particle volume fraction C enters in linearized momentum equations (11)–(13). It is a very significant complication of the stability problem, as compared to that for a dusty-gas flow, where the linearized continuity equation for the particle mass concentration is decoupled from the momentum equations [4].

We consider small disturbances to the main flow in the form of traveling waves (normal modes):

$$\mathbf{Q}(x, y, z, t) = \mathbf{q}(y) \exp\{i(k_x x + k_z z) + \sigma t\},$$

$$\mathbf{Q} = \{v, \omega, u_s, v_s, w_s\}. \quad (15)$$

Here, k_x and k_z are wave numbers in the x and z directions, respectively; $\sigma = \sigma_r + i\sigma_i$ is the complex amplification factor, so that σ_r determines the temporal growth or decay of the disturbance and σ_i is the phase velocity.

By eliminating the pressure from system (10)–(13) and using the nondivergence of the suspension velocity, we obtain the following three ordinary differential equations in terms of the amplitudes of the disturbances of the normal velocity v , the normal vorticity $\omega(y) = ik_z u(y) - ik_x w(y)$, and the particle

volume fraction $C(y)$:

$$\begin{aligned} & \frac{1}{\text{Re}} \left\{ \left(1 + \frac{5}{2} C_0 \right) (v^{IV} - 2k^2 v'' + k^4 v) \right. \\ & \quad + 5C_0'(v''' - k^2 v') + \frac{5}{2} C_0''(v'' + k^2 v) \\ & \quad \left. - ik_x \frac{5}{2} (U''' C + 2U'' C' + U' [C'' + k^2 C]) \right\} \\ & \quad + ik_x (\eta - 1) C_0'(U' v - U v') \\ & \quad + ik_x \rho_m (v U'' - U [v'' - k^2 v]) \\ & = \sigma (\rho_m [v'' - k^2 v] + (\eta - 1) C_0' v'), \end{aligned} \quad (16)$$

$$\begin{aligned} & \frac{1}{\text{Re}} \left(1 + \frac{5}{2} C_0 \right) (\omega'' - k^2 \omega) - ik_x \rho_m U \omega \\ & \quad + \frac{5}{2} C_0' \omega' - ik_z \rho_m U' v + \frac{ik_z}{\text{Re}} \frac{5}{2} (U' C)' = \sigma \rho_m \omega, \end{aligned} \quad (17)$$

$$-ik_x U C - v C_0' = \sigma C, \quad k^2 = k_x^2 + k_z^2. \quad (18)$$

Boundary conditions (14) take the form

$$v(y = \pm 1) = 0, \quad v'(y = \pm 1) = 0, \quad \omega(y = \pm 1) = 0. \quad (19)$$

In the limit of pure-fluid flow $C_0 \rightarrow 0$, $\eta \sim 1$, Eqs. (16) and (17) turn into the Orr-Sommerfeld and Squire equations, respectively [13], while in the limit $C_0 \rightarrow 0$, $C\eta \sim 1$ one obtains the equations describing the evolution of small disturbances in the dusty-gas flow with a nonuniform particle concentration [20].

The solution to the eigenvalue problem (16)–(18) provides the countable set of normal modes:

$$\{\sigma_n, \mathbf{q}_n(y)\}, \quad \mathbf{q}_n\{v_n, \omega_n, C_n\}, \quad (20)$$

where the modes are sorted by decreasing growth rate $\sigma_{r,n}$ with an increase in their number n . Any periodic solution of system (16)–(18) for a certain set of governing parameters Re , α , η , ζ , ξ , k_x , k_z is decomposed into the series of normal modes [12]:

$$\mathbf{Q}(x, y, z, t) = \sum_{n=1}^M \gamma_n \mathbf{q}_n(y) \exp\{i(k_x x + k_z z) + \sigma_n t\}. \quad (21)$$

Here, complex coefficients $\{\gamma_n\}$ determine the spectral projection of a disturbance with the wave numbers k_x , k_z and M is the sufficiently large number of modes.

We consider the suspension flow at small particle mass loadings $\alpha \sim 0.01$, so that the density of kinetic energy of the dispersed phase is small. Accordingly, we consider the kinetic energy of the carrier fluid E as the norm, determining the temporal growth of a disturbance (21):

$$E(\gamma, t) = \frac{1}{2ab} \int_{-a/2}^{a/2} \int_{-1}^1 \int_{-b/2}^{b/2} (u_r^2 + v_r^2 + w_r^2) dx dy dz. \quad (22)$$

Here, u_r , v_r , and w_r are real parts of the suspension velocity disturbances, $a = 2\pi/k_x$, $b = 2\pi/k_z$. After the expression of u_r , v_r , and w_r in terms of v and ω , the following relation is obtained [13]:

$$E(\gamma, t) = \frac{1}{8} \int_{-1}^1 \left[v^* v + \frac{1}{k^2} \left(\frac{dv^*}{dy} \frac{dv}{dy} + \omega^* \omega \right) \right] dy. \quad (23)$$

Here, the asterisk denotes complex conjugation. A combination of normal modes (21) with the spectral projection γ , which maximizes the kinetic energy (23) under the assumption of unit initial energy, is the optimal disturbance over a time interval t :

$$E(\gamma, t) \rightarrow E_{\max}, \quad E(\gamma, 0) = 1. \quad (24)$$

The global optimal disturbances are found by the energy maximization, not only over the spectral projection (24) (which is identical to the optimization over the initial conditions), but also over time t and the wave numbers k_x , k_z .

IV. PRELIMINARY ANALYSIS OF OPTIMAL GROWTH

Consider the time evolution of kinetic energy of a small disturbance of the suspension flow described by linearized equations (10)–(13). The corresponding equation is obtained by multiplying linearized momentum equations (11)–(13) by the corresponding velocity components and integrating over a flow domain V_f determined by

$$(x, y, z) \in [-L_x, L_x] \times [-1, 1] \times [-L_z, L_z],$$

where L_x and L_z are sufficiently large.

We restrict the analysis to the periodic disturbances $\mathbf{Q} = \{u, v, w, p, C\}$ in x and z directions, so that the following relations are valid:

$$\mathbf{Q}(-L_x, y, z, t) = \mathbf{Q}(L_x, y, z, t),$$

$$\mathbf{Q}(x, y, -L_z, t) = \mathbf{Q}(x, y, L_z, t).$$

As a result of the integration, the following equation for the kinetic-energy evolution is obtained:

$$\begin{aligned} \frac{\partial E}{\partial t} & = -2 \int_V \rho_m u v U' dV - \frac{5}{\text{Re}} \int_V \left[(U' C)' u + U' v \frac{\partial C}{\partial x} \right] dV \\ & \quad - \frac{5}{\text{Re}} \int_V C_0'' v^2 dV - \frac{2}{\text{Re}} \int_V \left(1 + \frac{5}{2} C_0 \right) \\ & \quad \times (|\nabla u|^2 + |\nabla v|^2 + |\nabla w|^2) dV, \\ E & = \int_V \rho_m (u^2 + v^2 + w^2) dV, \quad \rho_m = 1 - C_0 + C_0 \eta. \end{aligned} \quad (25)$$

The first integral on the right-hand side of Eq. (25) describes the energy transfer between the main shear flow and the Reynolds stresses generated by the small disturbances. The other terms describe viscous dissipation in the flow with a nonuniform viscosity. Note that the second and third terms are specific of the suspension flow with a nonuniform distribution of particles with a finite volume fraction (which results in a disturbance of the suspension viscosity and a variation of the suspension velocity profile). These terms vanish in the flow with a uniform particle concentration distribution. The new terms involve the disturbances to the streamwise u and the normal v velocity components, as well as the disturbance to the particle concentration C .

Consider now the flow of suspension with a uniform particle concentration distribution $C_0 = \text{const}$. It follows from the linearized continuity equation for particles (10) that $C \equiv 0$, so the second and third integrals in (25) are eliminated. If we divide the resulting equation by the initial energy to analyze the normalized energy growth, we obtain that the difference

between the suspension energy growth and that of the pure fluid is in the dissipative term involving the modified Reynolds number Re_s :

$$Re_s = Re \frac{1 - C_0 + C_0 \eta}{1 + 5/2 C_0}. \quad (26)$$

The analysis of expression (26) shows that an increase in C_0 results in an increase in Re_s for $\eta > 3.5$ and a decrease in Re_s for $\eta < 3.5$. Therefore, at a fixed particle mass concentration $C_0 \eta$, the minimum viscous dissipation is gained by the dusty-gas flow ($C_0 \ll 1$), while an increase in C_0 would result in an increase in viscous dissipation and a decrease in the energy growth.

V. NUMERICAL ALGORITHM AND VALIDATION

The numerical solution of eigenvalue problem (16)–(18) is carried out using a finite-difference method on a uniform grid with a nine-point stencil to increase the order of approximation and reduce the number of grid points N . The resulting eigenvalue problem for matrices is solved using the QR algorithm. The details of the numerical algorithm can be found in [20].

Since our main aim is to consider the flow with a nonuniform distribution of the particle volume fraction, we performed the test calculations to find the optimum mesh size which would provide the required accuracy. As a reference solution, we used that obtained by the orthonormalization method, which was developed earlier and applied to stability problems of a number of particle-laden flows, including the modal stability of a stratified suspension flow in a plane channel [8]. The method allows us to efficiently calculate the parameters of a single mode. We obtained that the eigenvalues of system (16)–(18) are calculated with high accuracy, even with $N = 300$ grid points at $\xi \geq 0.1$ (see Table I).

The optimal disturbances are found using the Lagrange multiplier method. The corresponding Euler-Lagrange equations formulated in terms of the spectral projection γ reduce the maximization problem (24) to a generalized eigenvalue problem for matrices [13]. The important condition of the calculation of optimal disturbances is the convergence in terms of the number of normal modes M in expansion (21). The test calculations showed that the required accuracy is achieved already for $M = 200$ modes (Table II).

VI. RESULTS AND DISCUSSION

A. Modal stability

The analysis of the modal stability of suspension flow in a plane channel was carried out in [8] for a particle concentration

TABLE I. Amplification factor σ for the most unstable mode at $Re = 5000$, $\alpha = 0.01$, $\eta = 1$, $\xi = 0.1$, $\zeta = 1$, $k_x = 1.1$, $k_z = 0$.

Method	σ_r	σ_i
$N = 200$	0.021 099 58	−0.292 491 26
$N = 400$	0.021 073 12	−0.292 469 18
Orthonormalization method [8]	0.021 073 08	−0.292 469 18

TABLE II. Dependence of the energy of optimal disturbances E on the number of normal modes M in expansion (21): $Re = 5000$, $\alpha = 0.01$, $\eta = 1$, $\xi = 0.1$, $\zeta = 1$, $k_x = 0$, $k_z = 2.2$, $t = 285$.

M	E
50	2452.9
100	2490.7
200	2496.6

profile mimicking the particle migration from the channel walls to the core region of the flow. Below we present a brief analysis of the growth rate of the first mode calculated for different sets of governing parameters with the aim to provide the basis for a nonmodal instability study. For details related to modal instability of a stratified suspension flow with finite-inertia particles, the readers are advised to refer to the study [8].

At the essentially subcritical Reynolds number $Re = 2500$, the flow is stable for any location of the particle layer (Fig. 2). With an increase in the Reynolds number to $Re = 5000$, the effect of the particles on the flow stability increases (Figs. 3 and 4). As shown in [7], the growth rate of the first mode is discontinuous in the vicinity of $\sigma_r = 0$ due to the singularity in the linearized continuity equation for the dispersed phase (18). This is confirmed by the calculations [Figs. 3 and 4(a)]. On the range of parameters considered, the flow is most unstable at $\eta = 1$, and when the particle layers are located in the vicinity of the walls [Figs. 3(a), 3(c), and 4(a)]. The instability typically increases with a decrease in the particle layer width at a fixed average particle mass concentration. [Compare curves 4 in Figs. 3(a) and 4(a), and curves 3 in Figs. 3(c) and 4(c).]

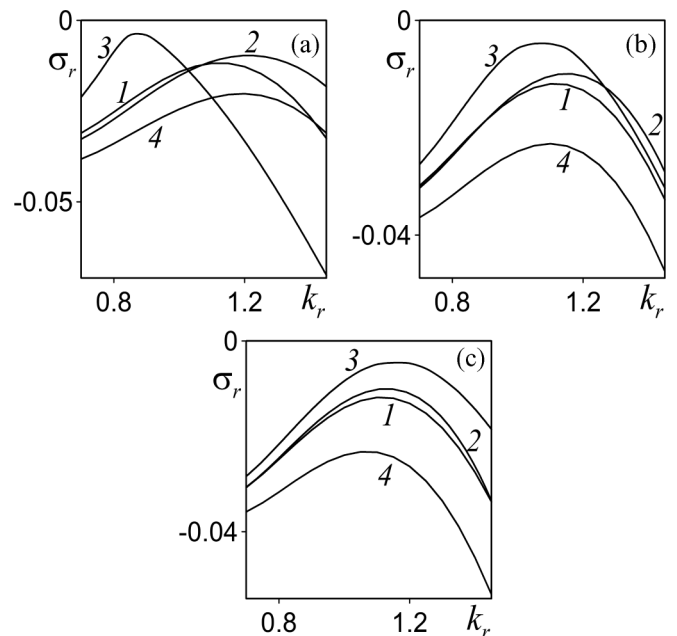


FIG. 2. Growth rate σ_r of the first two-dimensional mode against the wave number k_x for different locations of the particle layer ζ . Curves 1–4 correspond to $\zeta = 0, 0.6, 0.8$, and 1 , respectively. $Re = 2500$, $\alpha = 0.01$, $\eta = 1$, $\xi = 0.1$, $\zeta = 1$, $k_z = 0$.

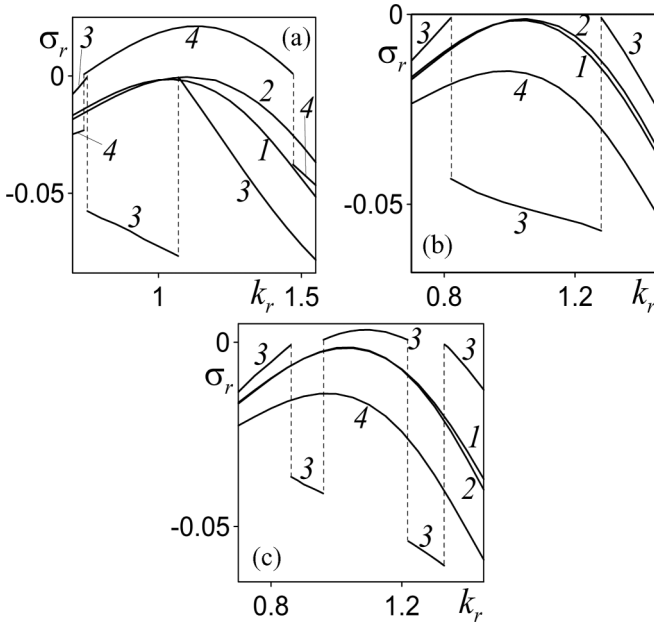


FIG. 3. Growth rate σ_r of the first two-dimensional mode against the wave number k_x for different locations of the particle layer ζ . Curves 1–4 correspond to $\zeta = 0, 0.6, 0.8$, and 1 , respectively. $\text{Re} = 5000$, $\alpha = 0.01$, $\eta = 1$, $\xi = 0.1$, $\zeta = 1$, $k_z = 0$.

B. Algebraic instability and transient growth

A parametric study of optimal disturbances was carried out. It is found that the transient growth in the suspension flow with a small average mass concentration of particles ($\alpha = 0.01$) and particle substance density $\eta \sim 1$ is amplified significantly as compared to the particle-free flow (see Fig. 5). In particular,

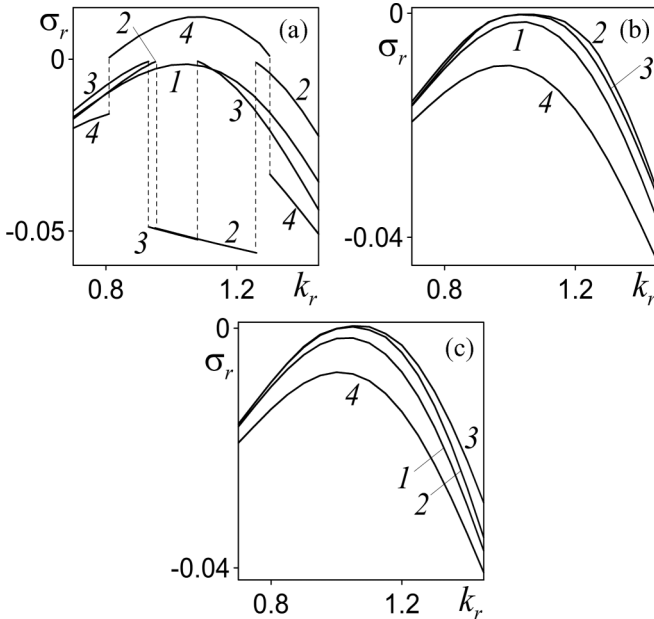


FIG. 4. Growth rate σ_r of the first two-dimensional mode against the wave number k_x for different locations of the particle layer ζ . Curves 1–4 correspond to $\zeta = 0, 0.6, 0.8$, and 1 , respectively. $\text{Re} = 5000$, $\alpha = 0.01$, $\eta = 1$, $\xi = 0.2$, $\zeta = 1$, $k_z = 0$.

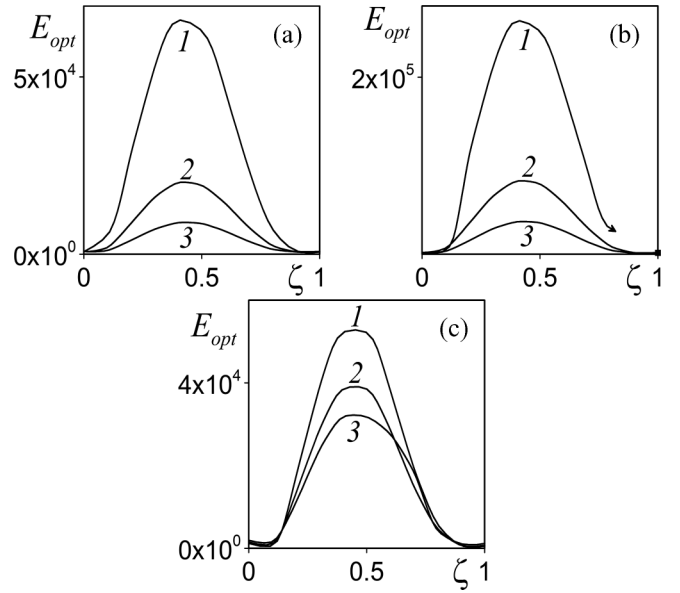


FIG. 5. Energy of global optimal disturbance E_{opt} against the location of particle layer ζ for $\text{Re} = 2500$, $\xi = 0.1$ (a), $\text{Re} = 5000$, $\xi = 0.1$ (b), and $\text{Re} = 5000$, $\xi = 0.2$ (c). Curves 1–3 correspond to $\eta = 1, 3$, and 10 , respectively. $\alpha = 0.01$.

for $\text{Re} = 5000$, $\eta = 1$, $\xi = 0.1$, the maximum energy of the optimal disturbance over the particle layer position ζ is found to be 2.73×10^6 , which is almost 3 orders of magnitude larger than that reported for the particle-free fluid flow in a plane channel ($E_{opt} \sim 4897$ at $k_x = 0$, $k_z = 2.044$ [13]). Note that the maximum optimal energy for a dusty-gas flow calculated in [20] at $\text{Re} = 5000$, $\xi = 0.1$, and a much larger average particle mass concentration $\alpha = 0.1$, is around 7.5×10^3 . The largest transient growth is gained by the suspension flow with the particle layers located in the middle between the channel walls and the axis ($\zeta \sim 0.4$), similar to the dusty-gas flow [20].

An increase in the particle layer width at a fixed average particle mass concentration results in a decrease in the energy of optimal disturbances [see Figs. 5(b) and 5(c)]. This is in agreement with the study of optimal disturbances to the dusty-gas flow in a plane channel with similar particle concentration distribution in the main flow [20].

Analysis of results presented in Fig. 5 also shows that the energy of optimal disturbances is scaled as Re^2 in the whole range of governing parameters, which is the result of a “lift-up” (or “vortex-tilting”) algebraic instability mechanism [12,13].

TABLE III. Energy of optimal disturbances to the particle-laden flow with a uniform particle concentration distribution for different values of Re and η calculated at $\alpha = 0.01$. $\eta = \infty$ corresponds to the dusty-gas flow, and $\alpha = 0$ the particle-free flow. $k_x = 0$, $k_z = 2.044$.

$\eta \setminus \text{Re}$	2500	5000
1	1176	4704
3	1232	4925
10	1252	5006
∞	1261	5041
$\alpha = 0$	1225	4898

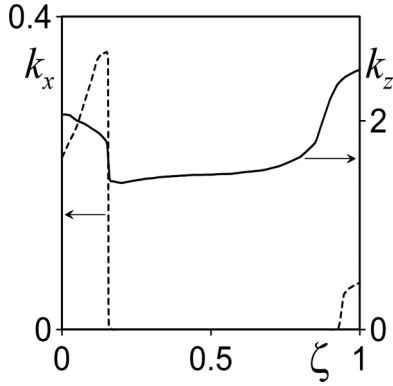


FIG. 6. Streamwise k_x (broken curve, left axis) and transverse k_z (strong curve, right axis) wave numbers of optimal disturbances against the location of the particle layer ζ for $Re = 5000$, $\alpha = 0.01$, $\eta = 1$, $\xi = 0.2$.

We also note a significant decrease in the energy of the optimal disturbances in the suspension flow, as compared to the pure-fluid and dusty-gas flows, when the particles are accumulated either in the vicinity of the channel walls ($\zeta > 0.9$) or near the channel axis ($\zeta < 0.1$).

Note that the growing modes are found at the set of parameters corresponding to the curve 3 in Fig. 5(b); therefore we plotted the dependence of the energy of optimal disturbances

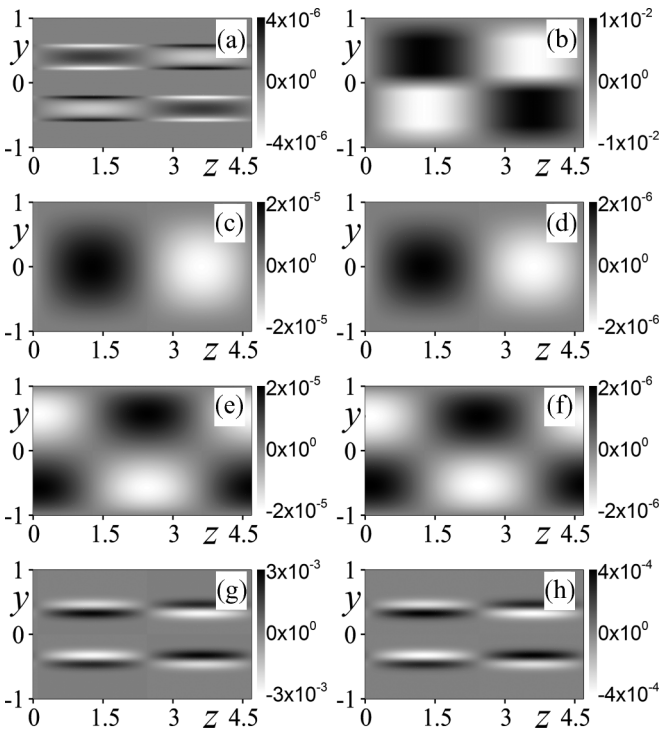


FIG. 7. Distribution of global optimal-disturbance velocity components u (a, b), v (c, d), w (e, f) and the optimal disturbance to the particle concentration C (g, h) in the y, z plane at initial time instant $t = 0$ (left column) and at optimal time instant $t = 1035$ (right column). $Re = 5000$, $\alpha = 0.01$, $\eta = 1$, $\zeta = 0.4$, $\xi = 0.1$, $k_x = 0$, $k_z = 1.34$.

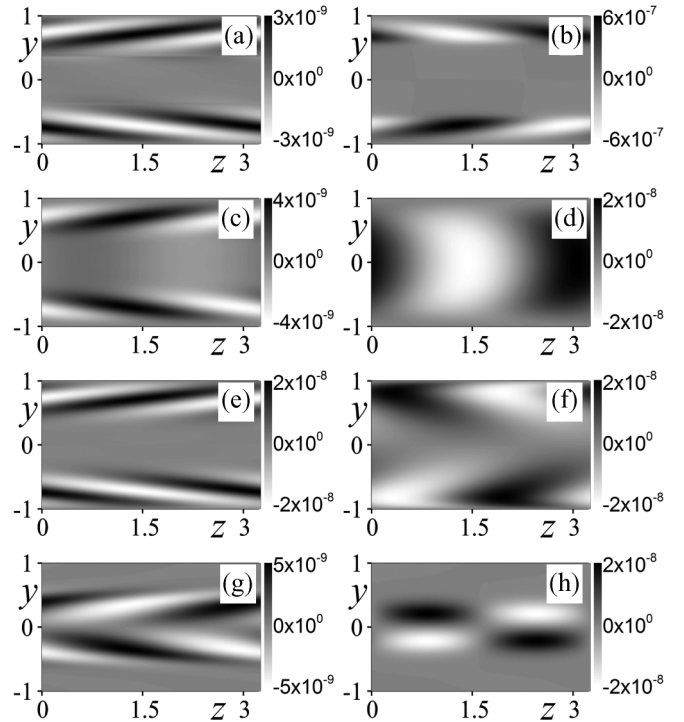


FIG. 8. Distribution of global optimal-disturbance velocity components u (a, b), v (c, d), w (e, f) and the optimal disturbance to the particle concentration C (g, h) in the y, z plane at initial time instant $t = 0$ (left column) and at optimal time instant $t = 1035$ (right column). $Re = 5000$, $\alpha = 0.01$, $\eta = 1$, $\zeta = 0.1$, $\xi = 0.2$, $k_x = 0.32$, $k_z = 1.93$.

on the location of the particle layer ζ only in the region where all modes decay ($\zeta < 0.82$).

The calculations of optimal energy growth in a suspension flow with a uniform particle concentration distribution showed that an increase in the particle-to-carrier fluid density ratio η at the fixed particle mass concentration α leads to a decrease in the transient growth (Table III). This is in agreement with the *a priori* analytical results on the evolution of kinetic energy of small disturbances presented in Sec. IV and the study presented in [22]. The qualitatively opposite result is obtained for the energy of the optimal disturbances in the stratified suspension flow at $0.1 < \zeta < 0.9$, namely, a decrease in the particle-to-carrier fluid substance density ratio η at a fixed average particle mass loading α results in the increase of the optimal-disturbance energy. It is attributable to the action of additional energy-transfer terms, arising due to the nonuniformity of the particle concentration in (25).

A significant difference between the transient growth in the dusty-gas and suspension flows is in the shape of disturbances. For the former flow, the shape of optimal disturbances is independent of the particle distribution [19,20]: global optimal disturbances are streaks with $k_x = 0$, $k_z = 2.044$. As is clear in Fig. 6, in the suspension flow the optimal wave number k_z depends on the location of the particle layer. Maximum values ($k_z > 2$) are obtained for $\zeta \leq 0.1$ and $\zeta \geq 0.8$ (particle layers are located near the channel axis or near the walls), whereas the minimum values of $k_z \sim 1.5$ correspond to $0.1 < \zeta < 0.8$. Another significant difference between the pure-fluid

TABLE IV. Distribution of kinetic energy among the velocity components of optimal disturbance shown in Fig. 7. Values are normalized by the total kinetic energy. $Re = 5000$, $\alpha = 0.01$, $\eta = 1$, $\zeta = 0.4$, $\xi = 0.1$, $k_x = 0$, $k_z = 1.34$.

Time	$\ u\ $	$\ v\ $	$\ w\ $
0	1.38×10^{-2}	3.7×10^{-1}	0.615
1035	~ 1	$< 10^{-7}$	$< 10^{-7}$

flow and the dusty-gas flow is in the nonzero streamwise wave number of the optimal disturbance: the largest value obtained in the calculations presented in Fig. 6 is $k_x = 0.35$ for $Re = 5000$, $\eta = 1$, $\zeta = 0.2$. Note that the corresponding transverse wave number k_z is 1.93, so the optimal disturbances are still elongated in the streamwise direction. Yet for a wide range of particle layer locations ($0.2 < \zeta < 0.8$), the optimal disturbances are independent of the x coordinate ($k_x = 0$).

As shown in Figs. 3 and 4, there is an unstable two-dimensional normal mode at $Re = 5000$; therefore it is straightforward to compare the modal and nonmodal growth. The maximum modal growth rate of the $\sigma_r = 0.0212$ is gained at $\xi = 0.1$, $\zeta = 1$ [see Fig. 3(a), curve 4]. The energy of the three-dimensional optimal disturbance calculated for the same set of governing parameters is $E_{opt} = 2496$, and the corresponding optimal time is $t = 286$. The calculation of the modal growth [$\exp(\sigma_r t)$] at the same time instant gives ≈ 430 , which is well below the transient growth predicted by the nonmodal theory.

The typical shapes of streamwise-independent and streamwise-dependent optimal disturbances are presented in Figs. 7 and 8, respectively. The distribution of kinetic energy among the velocity components is presented in Tables IV and V. Initially, the major portion of the kinetic energy is stored in the v - and w -velocity components of the optimal disturbance, while to the optimal time instant, the kinetic energy is transferred to the streamwise velocity component u . This behavior of the kinetic energy is the feature of the “lift-up” algebraic instability mechanism [12]. Note that the optimal disturbance of the particle concentration is localized in the particle layer [see Figs. 7(g) and 7(h), 8(g) and 8(h)].

TABLE V. Distribution of kinetic energy among the velocity components of optimal disturbance shown in Fig. 8. Values are normalized by the total kinetic energy. $Re = 5000$, $\alpha = 0.01$, $\eta = 1$, $\zeta = 0.1$, $\xi = 0.2$, $k_x = 0.32$, $k_z = 1.93$.

Time	$\ u\ $	$\ v\ $	$\ w\ $
0	2.88×10^{-2}	4.41×10^{-2}	0.927
64.4	0.963	3.29×10^{-3}	3.33×10^{-2}

VII. CONCLUSIONS

In the limit of negligibly small particle inertia, the transient growth of disturbances of a suspension flow in a plane channel is analyzed. The case is considered when in the main flow the particles are accumulated in two Gaussian layers, symmetric about the channel axis. It is found that the particles significantly modify the growth rate of the most unstable normal mode. The most pronounced destabilizing effect is produced by the particles located in the vicinity of the channel walls. The nonmodal instability analysis showed that on a wide range of governing parameters, taking into account a finite volume fraction of the particles results in a significant amplification of the transient growth of small disturbances. The maximum amplification is obtained for a suspension flow with the particle layers located in the middle between the channel walls and the flow axis, when the energy of the global optimal disturbances is up to 3 orders of magnitude larger than that in dusty-gas or pure-fluid flows. Over the entire range of governing parameters, the optimal disturbances have the shape of streaks elongated in the streamwise direction. In contrast to the dusty-gas flow, the wave numbers of the optimal disturbances depend on the particle layer location. When the particles are accumulated in the vicinity of the walls and near the channel axis, the optimal disturbance is streamwise dependent. In the range of flow parameters for which the first normal mode is unstable, the energy growth of the optimal disturbance is greater than that associated with the exponential growth of the first mode, and we may conclude that the transient growth (nonmodal mechanism) dominates the suspension flow instability.

ACKNOWLEDGMENT

This research was supported by the Russian Foundation for Basic Research (Grant No. 14-01-00147).

-
- [1] J.-P. Matas, J. F. Morris, and E. Guazelli, Transition to Turbulence in Particulate Pipe Flow, *Phys. Rev. Lett.* **90**, 014501 (2003).
- [2] P. G. Drazin and W. H. Reid, *Hydrodynamic Stability*, 2nd ed. (Cambridge University Press, Cambridge, UK, 1983).
- [3] P. J. Schmid and D. S. Henningson, *Stability and Transition in Shear Flows* (Springer-Verlag, New York, 2001).
- [4] P. G. Saffman, On the stability of laminar flow of a dusty gas, *J. Fluid Mech.* **13**, 120 (1962).
- [5] V. Ya. Rudyak, E. B. Isakov, and E. G. Bord, Hydrodynamic stability of the poiseuille flow of dispersed fluid, *J. Aerosol Sci.* **2**, 53 (1997).
- [6] S. A. Boronin and A. N. Osipov, Stability of a disperse-mixture flow in a boundary layer, *Fluid Dyn.* **43**, 66 (2008).
- [7] S. A. Boronin, Investigation of the stability of a plane-channel suspension flow with account for finite particle volume fraction, *Fluid Dyn.* **43**, 873 (2008).
- [8] S. A. Boronin, Hydrodynamic stability of stratified suspension flow in a plane channel, *Doklady Phys.* **54**, 536 (2009).

- [9] E. S. Asmolov and S. V. Manuilovich, Stability of a dusty-gas laminar boundary layer on a flat plate, *J. Fluid Mech.* **365**, 137 (1998).
- [10] T. Ellingsen, Stability of linear flow, *Phys. Fluids* **18**, 487 (1975).
- [11] M. L. Landahl, A note on algebraic instability of inviscid parallel shear flows, *J. Fluid Mech.* **98**, 243 (1980).
- [12] P. J. Schmid, Nonmodal stability theory, *Annu. Rev. Fluid Mech.* **39**, 129 (2007).
- [13] K. Butler and B. Farrel, Three-dimensional optimal perturbations in viscous shear flows, *Phys. Fluids A* **4**, 1637 (1992).
- [14] E. Reshotko and A. Tumin, Spatial theory of optimal disturbances in a circular pipe flow, *Phys. Fluids* **13**, 991 (2001).
- [15] A. Tumin and E. Reshotko, Spatial theory of optimal disturbances in boundary layers, *Phys. Fluids* **13**, 2097 (2001).
- [16] O. Levin, V. G. Chernoray, L. Löfdahl, and D. S. Henningson, A study of the Blasius wall jet, *J. Fluid Mech.* **539**, 313 (2005).
- [17] S. A. Boronin, J. J. Healey, and S. S. Sazhin, Non-modal stability of round viscous jets, *J. Fluid Mech.* **716**, 96 (2013).
- [18] P. H. Alfredsson, A. A. Bakchinov, V. V. Kozlov, and M. Matsubara, Laminar-turbulent transition at a high level of free stream turbulence, in *Nonlinear Instability and Transition in Three-Dimensional Boundary Layers*, edited by P. W. Duck and P. Hall (Dordrecht, Kluwer, 1996), pp. 423–436.
- [19] J. Klinkenberg, H. C. de Lange, and L. Brandt, Modal and non-modal stability of particle-laden channel flow, *Phys. Fluids* **23**, 064110 (2011).
- [20] S. A. Boronin, Optimal perturbations in dusty-gas plane-channel flow with a non-uniform distribution of particles, *Fluid Dyn.* **47**, 351 (2012).
- [21] S. A. Boronin and A. N. Osipov, Modal and non-modal stability of dusty-gas boundary layer flow, *Fluid Dyn.* **49**, 770 (2014).
- [22] J. Klinkenberg, H. C. de Lange, and L. Brandt, Linear stability of particle laden flows: The influence of added mass, fluid acceleration and Basset history force, *Meccanica* **49**, 811 (2014).
- [23] S. A. Boronin, Stability of plane Couette dispersed flow with a finite volume fraction of inclusions, *Fluid Dyn.* **46**, 64 (2011).
- [24] G. Segre and A. Silbereberg, Behavior of macroscopic rigid spheres in a Poiseuille flow, Part 2. Experimental results and interpretation, *J. Fluid Mech.* **14**, 136 (1962).
- [25] J.-P. Matas, J. F. Morris, and E. Guazzelli, Inertial migration of rigid spherical particles in Poiseuille flow, *J. Fluid Mech.* **515**, 171 (2004).
- [26] F. E. Marble, Dynamics of dusty gases, *Annu. Rev. Fluid Mech.* **2**, 397 (1970).